

Efficient simulation of optical nonlinear cavity circuits

Thomas Van Vaerenbergh · Martin Fiers ·
Joni Dambre · Peter Bienstman

Received: 25 September 2014 / Accepted: 14 January 2015 / Published online: 25 January 2015
© Springer Science+Business Media New York 2015

Abstract Recently, we proposed a node-based framework that can be used to simulate large circuits of nonlinear photonic components both in the time-domain and in the frequency-domain. In that framework, components are described using a flexible and very general ‘node’-definition, allowing to simulate circuits that contain a wide variety of components with different physical effects. In this paper, we extend the node-definition of this framework such that the linear coupling between access waveguides and resonance states in optical resonators can be more explicitly incorporated, reducing the simulation time in large-scale cavity circuits.

Keywords Modeling · Nanophotonics · Integrated circuits

1 Introduction

Many optical resonators can be described using a Coupled Mode Theory (CMT)-like format for the equations concerning the optical field. For instance, the models that are used to describe the dynamics of a passive nonlinear microring (Van Vaerenbergh et al. 2012; Fiers et al. 2014) or a microdisk laser (Alexander et al. 2013; Van Vaerenbergh et al. 2013), are CMT-based.

This work is supported by the Human Brain Project, the IAP Photonics@be of the Belgian Science Policy Office and the ERC NaResCo Starting grant. T.V.V. is supported by the Flemish Research Foundation (FWO) for a Ph.D. Grant.

T. Van Vaerenbergh (✉) · P. Bienstman
Photonics Research Group, INTEC, Ghent University - imec, Sint-Pietersnieuwstraat 41,
9000 Ghent, Belgium
e-mail: thomas.vanvaerenbergh@intec.ugent.be

M. Fiers
Luceda Photonics, Noordlaan 21, 9200 Dendermonde, Belgium
URL: <http://www.lucedaphotonics.com>

J. Dambre
Computer Systems Lab, ELIS, Ghent University, Sint-Pietersnieuwstraat 41, 9000 Ghent, Belgium

In this paper we will point out how the node-based framework presented by [Fiers et al. \(2011\)](#) can be adapted to CMT-style models, and how this adaptation can sometimes significantly increase the simulation speed. For instance, the large-scale circuit simulations performed by [Fiers et al. \(2014\)](#) took advantage of this speed up.

2 Reshaping the system equation towards CMT

[Fiers et al. \(2011\)](#) derived the generalized connection matrix $C_{in,ex}$, which models the linear and instantaneous transmission of the waves that originate from a generalized ‘external’ sources vector $s_{ext}(t)$ and travel through the components of the circuit. This connection matrix speeds up the time-domain simulations when the inputs of all the memory-containing (MC) components (e.g., resonators or lasers) need to be calculated for a given $s_{ext}(t)$, as it eliminates the memoryless (ML) components (e.g., splitters or instantaneous waveguides) from the circuit. One single sparse matrix product

$$s_{in,MC}(t) = C_{in,ex}s_{ext}(t), \tag{1}$$

updates the inputs of the MC simultaneously for all the nodes. As this improvement in speed is clearly due to the *linearity* of the signal transfer encoded in the scatter-matrix, we will now investigate how additional linear behavior in the MC node can be exploited to make the framework even more efficient.

In CMT models, the coupling between the optical modes of the cavity and the access waveguides is also linear. Typically, the CMT equations of a nonlinear resonator i are given by:

$$\frac{da_i}{dt} = M_i a_i + K_i^T s_{i,in} + N_i(a, t, \dots) \tag{2}$$

The function N_i describes the nonlinear contribution, e.g., due to changes in absorption or refractive index by the Kerr nonlinearity. If the cavity model contains additional dynamic variables, such as the number of free carriers, or the temperature, these extra equations can as well be shoehorned in the previous matrix format, by extending K_i^T in the appropriate places with zeros and M_i with linear contributions of the corresponding ordinary differential equation (ODE), while the remaining nonlinear terms can be incorporated in $N_i(a, t, \dots)$. More generally, every MC component can be trivially transferred into this format, by extending the original ODE system with additional M_i , K_i^T and D_i matrices equal to zero. As we use sparse matrices, these additional zeros have no significant influence on the simulation speed.

Even if the resonator is nonlinear, the coupling of the modes and input signals to the output stays linear:

$$s_{i,out} = S_i s_{i,in} + D_i a, \tag{3}$$

We now define the linear coupling matrices M , K^T and D for the circuit as a whole. These matrices are block matrices, constructed from the submatrices M_i , K_i^T and D_i for all the MC nodes $i \in \{0, \dots, N - 1\}$. Using the same syntax as before, M linearly couples the states to the states, K^T couples the input to the states, while D couples the states to the output. If we suppose the system has s states and p ports, then M is $s \times s$ dimensional, while D and K are both $p \times s$ dimensional. Using those matrices, the total ODE of the circuit becomes:

$$\frac{da}{dt} = Ma + K^T s_{in,MC} + N(a, t, \dots) \tag{4}$$

The generalized source term defined by [Fiers et al. \(2011\)](#) can be split into two parts: a linear part, related to the linear coupling by D_i of the resonators in the circuit, and an external

source term $\mathbf{s}'_{ext}(t)$ of which the linear coupling terms are subtracted (e.g., containing the input signals of the sources in the circuit, or the outputs of waveguides with delay), such that:

$$\mathbf{s}_{in,MC} = \mathbf{C}_{in,ex} (\mathbf{D}\mathbf{a} + \mathbf{s}'_{ext}). \tag{5}$$

Interestingly, by doing this we already increased the flexibility of the framework. Indeed, whereas \mathbf{M} is originally considered to be a block-diagonal matrix, coupling only states within a node, we can now also extend it to directly couple states between different nodes, whereas in the previous formalism, only optical coupling through the ports was allowed. The current formalism, e.g., allows for a more generic way of implementing optical coupling between cavity modes, using the theory developed by Little et al. (1997). Also the implementation of thermal coupling between nearby resonators is conceptually simplified by this extension.

3 Increasing sparseness

In this section, we will use the knowledge of the positions of resonators, detectors and sources in a circuit to make the matrices in the system equations sparser, resulting in a speed improvement of the calculation time.

If a circuit contains cavities with a CMT model, we know that s'_{ext} will be equal to zero at those port positions. Similarly, port positions of detectors in the circuit will also correspond to additional zeros in s'_{ext} . We will now introduce a diagonal $p \times p$ matrix \mathbf{I}^M_{ex} , that contains a zero on the diagonal for each port that corresponds to a resonator or a detector. Using this matrix and Eq. (5), assuming that the rows of \mathbf{D} are only nonzero at the port positions of resonators we obtain:

$$\mathbf{s}_{in,MC} = \mathbf{C}_{in,ex} \left[(\mathbf{I} - \mathbf{I}^M_{ex}) \mathbf{D}\mathbf{a} + \mathbf{I}^M_{ex} \mathbf{s}'_{ext} \right]. \tag{6}$$

The presence of \mathbf{I}^M_{ex} in the previous equation generates additional zeros in the matrix products, making them more sparse and hence potentially speeding up the calculations. Here, \mathbf{I}^M_{ex} can be considered to be some kind of ‘mask’ matrix.

Additionally, when doing a time-domain simulation, it is not necessary to calculate $\mathbf{s}_{in,MC}$ at the port positions that contain sources (assuming that these sources are not influenced by reflected signals from the circuit, as is the case in most simulations). We will now introduce a second diagonal $p \times p$ mask matrix \mathbf{I}^M_{in} , that contains a zero on the diagonal for each port that corresponds to a resonator or a source. By defining $\mathbf{s}'_{in,MC} = \mathbf{I}^M_{in} \mathbf{s}_{in,MC}$ as the vector that monitors the inputs of all the ML nodes, except for the sources and the resonators, we can rewrite $\mathbf{s}_{in,MC}$ to:

$$\mathbf{s}_{in,MC} = \mathbf{s}'_{in,MC} + (\mathbf{I} - \mathbf{I}^M_{in}) \mathbf{s}_{in,MC}. \tag{7}$$

Assuming that only the columns of \mathbf{K}^T corresponding to the resonators are different from zero, $\mathbf{K}^T \mathbf{s}'_{in,MC} = 0$ and introduction of Eq. (7) in Eq. (4) gives:

$$\frac{d\mathbf{a}}{dt} = \mathbf{M}\mathbf{a} + \mathbf{K}^T (\mathbf{I} - \mathbf{I}^M_{in}) \mathbf{s}_{in,MC} + \mathbf{N}(\mathbf{a}, t, \dots). \tag{8}$$

Substitution of Eq. (6) results in:

$$\begin{aligned} \frac{d\mathbf{a}}{dt} = & \left[\mathbf{M} + \mathbf{K}^T (\mathbf{I} - \mathbf{I}^M_{in}) \mathbf{C}_{in,ex} (\mathbf{I} - \mathbf{I}^M_{ex}) \mathbf{D} \right] \mathbf{a} \\ & + \left[\mathbf{K}^T (\mathbf{I} - \mathbf{I}^M_{in}) \mathbf{C}_{in,ex} \mathbf{I}^M_{ex} \right] \mathbf{s}'_{ext} + \mathbf{N}(\mathbf{a}, t, \dots), \end{aligned} \tag{9}$$

while $\mathbf{s}'_{in,MC}$ can be calculated to be:

$$\mathbf{s}'_{in,MC} = [\mathbf{I}_{in}^M \mathbf{C}_{in,ex} (\mathbf{I} - \mathbf{I}_{ex}^M) \mathbf{D}] \mathbf{a} + [\mathbf{I}_{in}^M \mathbf{C}_{in,ex} \mathbf{I}_{ex}^M] \mathbf{s}'_{ext}. \tag{10}$$

In the previous two equations, we encounter four new matrices:

$$\left[\mathbf{M} + \mathbf{K}^T (\mathbf{I} - \mathbf{I}_{in}^M) \mathbf{C}_{in,ex} (\mathbf{I} - \mathbf{I}_{ex}^M) \mathbf{D} \right], \tag{11}$$

$$\left[\mathbf{K}^T (\mathbf{I} - \mathbf{I}_{in}^M) \mathbf{C}_{in,ex} \mathbf{I}_{ex}^M \right], \tag{12}$$

$$\left[\mathbf{I}_{in}^M \mathbf{C}_{in,ex} (\mathbf{I} - \mathbf{I}_{ex}^M) \mathbf{D} \right], \tag{13}$$

$$\left[\mathbf{I}_{in}^M \mathbf{C}_{in,ex} \mathbf{I}_{ex}^M \right]. \tag{14}$$

Dependent on the connection topology of the circuit, the first matrix can be dense, but the last three will generally be sparse. Furthermore, these matrices can be calculated in advance. Hence, in a time-domain simulation, integration of Eq. (9) can be done by updating only \mathbf{s}'_{ext} instead of \mathbf{s}_{ext} . Advantageously, \mathbf{s}'_{ext} will be more sparse, and additionally, the output signals at the resonators do not need to be tracked anymore, as their influence on the inputs of other non-resonator MC components is incorporated by the matrix product with \mathbf{a} in Eq. (10). Similarly, in circuits with a lot of resonators and sources, $\mathbf{s}'_{in,MC}$ is a lot sparser than $\mathbf{s}_{in,MC}$.

In principle, by incorporating additional stochastic contributions to emulate vacuum fluctuations in the source terms, our framework can be extended towards semiclassical simulations of large quantum optical circuits. Indeed, the previous equations can be conceptually mapped to the deterministic part of the stochastic differential equations that were proposed by Santori et al. (2014).

4 Applicability of the extended framework

Importantly, the previous derivation considered general circuits, that can contain other components than sources, detectors and resonators. Hence, components such as waveguides with delay or optical amplifiers can still be part of the circuit, making this extended framework very flexible.

Interestingly, the replacement of $\mathbf{C}_{in,ex}$ in Eq. (1) with its equivalent in Eq. (14) already offers a speed improvement in circuits without resonators, but with a significant number of detectors and sources. In this case, the matrices in Eq. (11)–(13) are dimensionless (i.e., the number of rows and/or columns is equal to zero) and, hence, do not slow down the calculation.

However, if we now consider circuits with a significant number of resonators, the speed gain depends both on the circuit topology and the cavity type.

In Fig. 1, we investigate the dependence of the simulation speed on the topology using two circuits with a significant number of resonators. In Fig. 1a, similar to Maes et al. (2009), we simulate chains of lossless inline Kerr-nonlinear PhC cavities. These inline cavities have a single standing wave mode and at resonance all light is transmitted, while far from resonance all light is reflected. For large chains, using the extended framework results in a $\sim 25\%$ -reduction in the number of non-zero elements in the matrix products. As a large part of the simulation time is spent in the calculation of these matrix products, this results in a significant decrease of the total simulation time. In Fig. 1b we simulate the large nanophotonic reservoir of PhC cavities proposed by Fiers et al. (2014). In this case, the relative reduction in calculation

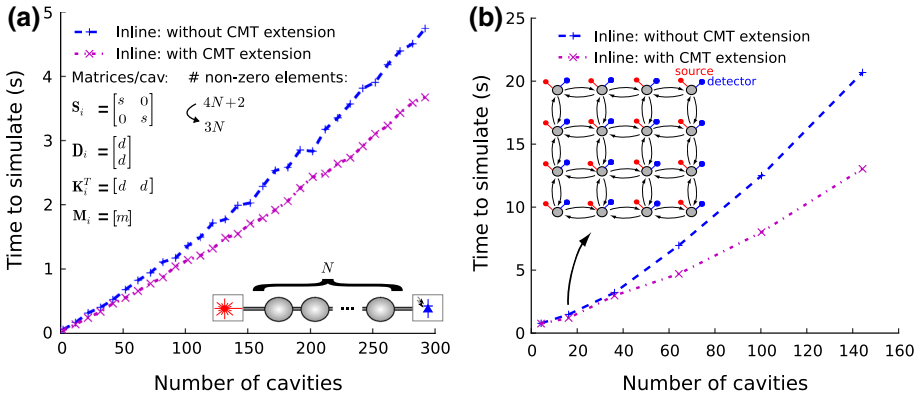


Fig. 1 (left) In a long chain of N inline PhC cavities, incorporation of the CMT formalism improves the simulation speed, due to a reduction of $4N + 2$ non-zero elements to $3N$ in the circuit matrix description. (right) A similar improvement can be seen in a simulation of a nanophotonic reservoir of inline PhC cavities in the same topology as discussed by Fiers et al. (2011, 2014). Similar to Fiers et al. (2011), a fixed integration stepsize of 0.1 ps is chosen and the input signals in both simulations are 10 ns long noise signals

time is even stronger. This is mainly due to the large number of sources and detectors in this nanophotonic reservoir, which brings along a lot of unnecessary calculations per time step in the original framework (e.g., propagating nonexistent output signals of the detectors to the sources).

In Fig. 2, we illustrate the influence of the cavity type on the simulation speed, by repeating the simulation performed in Fig. 1a, for two different cavity types: a unidirectional ring (we use a CMT-model of a ring, in which only one the two counterpropagating modes is explicitly incorporated) and a side-coupled PhC cavity (at resonance all light is reflected, far from resonance all light is transmitted). Clearly, the extended framework identifies the unidirectional nature of the ring-model and automatically reduces the number of non-zero matrix elements by 50%. Unfortunately, whereas the scatter matrix - which models the off-resonance behavior—of an inline PhC cavity only directly couples nearest neighbor cavities,

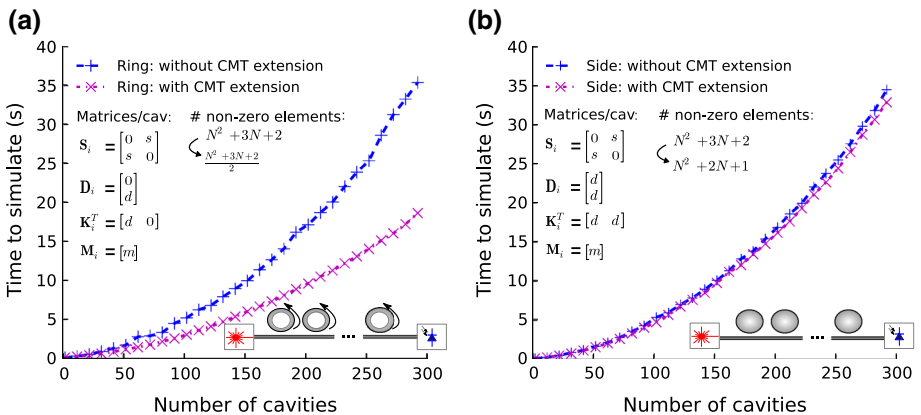


Fig. 2 Not only the circuit topology, but also the cavity type significantly influences the improvement of the simulation speed. In a chain of unidirectional Kerr-nonlinear rings, the extended framework automatically reduces the number of non-zero elements by 50% (left). In contrast, such a significant reduction can not be perceived for side-coupled PhC cavities (right). Simulation settings are similar to Fig. 1a

in the case of the side-coupled PhC chain, all the cavities of the chain are directly coupled to each other by their scatter-matrix. Consequently, this non-sparse coupling causes the matrix in Eq. (11) to be non-sparse as well, such that the extended framework only results in a negligible decrease in simulation time. Theoretically, for some resonator circuits, the CMT-approach can even result in less sparse circuit matrices, thereby increasing the simulation time. In these cases, this speed reduction can be mitigated by excluding the problematic resonators in the circuit (eg., having more states than ports and non-sparse \mathbf{K}_i^T and \mathbf{D}_i) out of the resonator list that is used to construct \mathbf{D} , \mathbf{K}^T , \mathbf{I}_{in}^M and \mathbf{I}_{ex}^M .

Finally, the extended framework also allows to analyse the CMT-resonances in the frequency domain. Indeed, the linear steady-state transmission of the circuit can be calculated by assuming $\mathbf{N}(\mathbf{a}, t, \dots) = 0$ and solving $\frac{d\mathbf{a}}{dt} = 0$ in Eq. (9).

5 Conclusion

By taking benefit of the linear part in the CMT-equations of optical resonators, the node-based framework proposed by Fiers et al. (2011) can be optimized for the simulation of large-scale resonator-circuits. Due to the use of sparse matrices, this results for some circuit topologies and cavity types in a significant speed increase.

References

- Alexander, K., Van Vaerenbergh, T., Fiers, M., Mechet, P., Dambre, J., Bienstman, P.: Excitability in optically injected microdisk lasers with phase controlled excitatory and inhibitory response. *Opt. Express* **21**, 28922–28932 (2013)
- Fiers, M., Van Vaerenbergh, T., Caluwaerts, K., Vande Ginste, D., Schrauwen, B., Dambre, J., Bienstman, P.: Time-domain and frequency-domain modeling of nonlinear optical components on circuit-level using a node-based approach. *J. Opt. Soc. Am. B* **29**(5), 896–900 (2011)
- Fiers, M., Van Vaerenbergh, T., Wyffels, F., Verstraeten, D., Schrauwen, B., Dambre, J., Bienstman, P.: Nanophotonic reservoir computing with photonic crystal cavities to generate periodic patterns. *IEEE Trans. Neural Netw. Learn. Syst.* **25**(1), 344–355 (2014)
- Little, B.E., Chu, S.T., Haus, H.A., Foresi, J., Laine, J.-P.: Microring resonator channel dropping filters. *J. Lightwave Technol.* **15**(6), 998–1005 (1997)
- Maes, B., Fiers, M., Bienstman, P.: Self-pulsing and chaos in series of coupled nonlinear micro-cavities. *Phys. Rev. B* **80**(1), 033805 (2009)
- Santori, C., Pelc, J.S., Beausoleil, R.G., Tezak, N., Hamerly, R., Mabuchi, H.: Quantum noise in large-scale coherent nonlinear photonic circuits. *Phys. Rev. Appl.* **1**(5), 054005 (2014)
- Van Vaerenbergh, T., Fiers, M., Mechet, P., Spuesens, T., Kumar, R., Morthier, G., Schrauwen, B., Dambre, J., Bienstman, P.: Cascadable excitability in microrings. *Opt. Express* **20**(18), 20292–20308 (2012)
- Van Vaerenbergh, T., Alexander, K., Dambre, J., Bienstman, P.: Excitation transfer between optically injected microdisk lasers. *Opt. Express* **21**(23), 28922–28932 (2013)